Eu(III)-Fulvic Acid Complexation Evidence of Fulvic Acid Concentration Dependent Interactions by Time-Resolved Luminescence Spectroscopy

Yasmine Z. Kouhail [†,‡], *Marc F. Benedetti* [†], *Pascal E. Reiller* [‡, §]

[†] Institut de Physique du Globe de Paris, Sorbonne Paris Cité, Université Paris Diderot, UMR 7154 CNRS, F-75005 Paris, France.

[‡] Commissariat à l'Énergie Atomique et aux énergies alternatives, CE Saclay, CEA, DEN, DANS, DPC, Laboratoire de développement Analytique Nucléaire Isotopique et Élémentaire, and [§] Université Paris-Saclay, Département de Chimie, Centre d'Étude du CEA de Saclay, Bâtiment 391 PC 33, F-91191 Gif-sur-Yvette Cedex, France.

Article published in

Environmental Science & Technology **2016**, 50 (7), 3706−3713.

DOI: 10.1021/acs.est.5b05456

1. Résumé

La spéciation de l'europium a été étudiée par spectrofluorimétrie laser à résolution temporelle (SLRT) en présence d'un acide fulvique de Suwannee river (SRFA). Deux comportements de luminescence d'Eu(III) ont été mis en évidence à partir des isothermes de complexations construites pour différentes concentrations en Eu(III), valeurs de pH, forces ioniques et concentrations en SRFA. Dans la première partie des isothermes, à faibles concentrations en SRFA, on observe l'évolution classique de la luminescence de l'europium lors de la complexation par les substances humiques. Le ratio d'asymétrie entre les transitions $^5D_0 \rightarrow {}^7F_2$ et $^5D_0 \rightarrow {}^7F_1$ augmente jusqu'à atteindre un plateau et une décroissance de luminescence biexponentielle – avec un temps de vie très court de l'ordre de quelques µs et un second temps de vie plus long que celui d'Eu^{3+} – est observée. A de plus fortes C_{SRFA}, un second mode de luminescence est mis en évidence où le ratio d'asymétrie continue d'augmenter après le plateau, ce qui peut être un signe de la formation d'un autre type de complexe, ou cela peut également refléter une organisation spatiale différente des complexes Eu-SRFA. Les temps de vie de luminescence continuent d'augmenter mais leur lien avec le nombre de molécules d'eau dans la première sphère de coordination de l'ion Eu^{3+} n'est pas simple du fait des mécanismes de quenching. L'évolution de l'environnement chimique de l'europium est également dépendante de la force ionique. Ces observations suggèrent qu'en plus d'interactions à courte distance – complexation intra-particulaire – il peut également y avoir des interactions à plus longue distance – répulsion inter-particulaire – entre les particules qui complexent l'europium aux fortes concentrations en SRFA. Ces interactions inter-particulaires ne sont pas prises en compte dans les différents modèles de complexation existants.

2. Abstract

Europium speciation is investigated by time-resolved luminescence spectroscopy (TRLS) in the presence of Suwannee River fulvic acid (SRFA). From complexation isotherms built at different total Eu(III) concentrations, pH values, ionic strength, and SRFA concentrations, it appears that two luminescence behaviors of Eu(III) are occurring. The first part, at the lowest C_{SRFA} values, is showing the typical luminescence evolution of Eu(III) complexed by humic substances—*i.e.* the increase of the asymmetry ratio between the $^5D_0 \rightarrow {}^7F_2$ and $^5D_0 \rightarrow {}^7F_1$ transitions up to a plateau—, and the occurrence of a bi-exponential decay—the first decay being faster than free Eu^{3+}. At higher C_{SRFA}, a second luminescence mode is detected as the asymmetry ratio is increasing again after the previous plateau, and could correspond to the formation of another type of complex, and/or it can reflect a different spatial organization of complexed europium within the SRFA structure. The luminescence decay keeps on evolving but link to hydration number is not straightforward due to quenching mechanisms. The Eu(III) chemical environment evolution with C_{SRFA} is also ionic strength dependent. These observations suggest that in addition to short range interactions—intra-particulate complexation—, there might be interactions at longer range—inter-particulate repulsion—between particles that are complexing Eu(III) at high C_{SRFA}. These interactions are not yet accounted by the different complexation models.

TOC ART

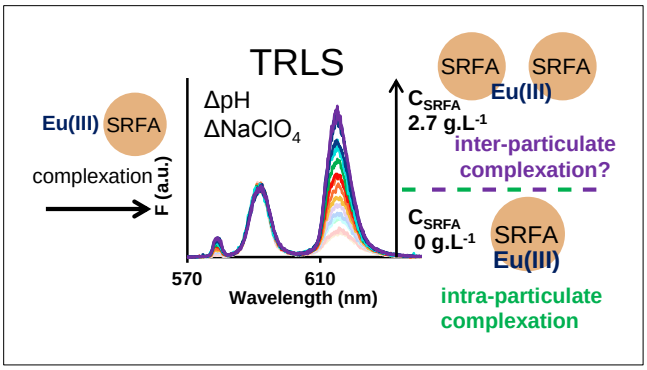

3. Introduction

The use of rare earths, and particularly the lanthanides (Ln), is increasing in modern industry.[1] Their importance in the understanding of geochemical processes, the presence of radioisotopes of lanthanides in spent nuclear fuels and radioactive wastes, and their analogy with some actinides (An) under the +III oxidation state, justify a better understanding of their environmental chemistry in waters, soils, and sediments.

Humic substances (HS), mainly composed of humic (HA) and fulvic (FA) acids are one of the main component of aquatic and soil ecosystems and are known to play an important role in the binding and transport of trace metals such as Ln(III).[2-4] Because of their strong interactions with surfaces[5] and their colloidal properties,[6] HS may affect Ln(III) either by supporting their mobility in water, or by limiting their migration in soils and sediments.

HS contain a great diversity of binding sites making it difficult to define equilibrium constants for each complexation reaction. This has led to a wide variety of models.[7] The most advanced models that permit to account for heterogeneity of HS, metal loading, pH, and ionic strength effects consider HS either as a mixture of discrete groups of sites—with different degree of correlations between these groups of sites—, *e.g.*, Model VI-VII,[8,9] or as a continuous distribution of groups of sites, *e.g.*, NICA-Donnan.[10] These kinds of models consider electrostatic phenomena, but the descriptions are somewhat different—hard sphere with a Donnan potential at the interface *vs.* permeable Donnan gel, respectively—when the structure of HS in general, and the structure of the Ln(III)-HS complexes in particular, remains largely under discussion.

Some Ln(III) and An(III) show a remarkable luminescence that is linked both to symmetry of their chemical environment,[11] and to the amount of water molecules in the first hydration sphere.[12,13] This information can be obtained both from the evolution of the luminescence spectrum and from the decay time. This has been the basis of a vast literature on the interaction between Ln-An(III) and HS.[14-27] Particularly, it has been shown that coordination structure around a metal ion is continuously modified by HS complexation when pH is varying.[20,28] Time resolution of the luminescence signal, through time-resolved luminescence spectroscopy (TRLS), was used to obtain complexation constants as well as structural properties.

The complexation strength of Ln(III) by HS can be considered relatively homogeneous within the series,[29-31] in agreement with the strong proportion of oxygen containing functionalities of HS.[30,32] Milne et al.[33,34] proposed generic complexation data for Ln(III) and An(III) in the framework of the NICA-Donnan model, but the great diversity of the reported studies, and the inherent heterogeneity of the different HS samples used throughout these studies led to some problems, particularly the proposed parameters for An(III), but also between Ln(III). As an example, Milne et al.[34] proposed different median affinity constants, $\log_{10}\tilde{K}_{M^{n+},i}$, for Am(III) and Cm(III), which is relatively surprising knowing the strong analogy between these two actinides(III), particularly regarding HS interactions.[18] The correlation between NICA-Donnan parameters—Figure 1 of Milne et al.[34]—and the first hydrolysis constants of the metals, $\log_{10}{}^*\beta^\circ_1$, also exemplify this problem: Am(III) and Cm(III) are supposed to have comparable $\log_{10}{}^*\beta^\circ_1 \approx -7$,[35] when Am(III) appears close to UO_2^{2+}—$\log_{10}{}^*\beta^\circ_1$ *viz.* -5.8 in Figure 1 of Milne et al.[34] and $\log_{10}{}^*\beta^\circ_1 = -5.25$ in Guillaumont et al.[35]. Furthermore, the particular interaction of HS with metals *vs.* pH, CO_3^{2-} and oxalate concentration, etc., led to the proposition of the formation of ternary complexes,[20,36-40] which are not always necessary to interpret experimental data within the framework of NICA-Donnan[23,25,41] or Model VI-VII,[42-44] but was sometimes proposed nevertheless.[39,40]

Cations are able to bridge two different polymer molecules,[45] and this supramolecular association increases with cation valence.[46] Supramolecular associations of HS are also known.[47] The effect of cations on these supramolecular structures was suggested[48] but needs further works.[49-52] Nevertheless, the effect of Eu(III) on the aggregation of HA was shown,[53-55] but the effect of HS concentration received little attention. There is therefore still a need for systematic studies of Ln(III)-HS complexation at varying pH, HS concentration, and ionic strength with spectroscopic information on the chemical environment of the metal.

Our aim is to propose an as comprehensive as possible study of the speciation of a trivalent luminescent lanthanide, Eu(III), in a wide parametric space in term of pH values, ionic strength, and HS concentration to better understand Ln(III)-NOM interactions and structures of NOM complexes with these trivalent cations. Time-resolved luminescence spectroscopy could be a useful tool to evidence the effect of the supramolecular structures on Eu(III)-NOM complexes since it provides information on Eu(III) environment. We will use the Suwannee River fulvic acid (SRFA), considered as a proxy of natural aquatic organic matter reactivity,[56] the relatively low UV-Visible absorption properties of which permits to use rather high concentration of FA in TRLS experiments compared to other HS extracts.[24] We will take

advantage of the luminescence properties of Eu(III) to characterize the Eu(III)-FA complexation and to evaluate its chemical environment using TRLS.

4. Materials and methods

4.1. Reagents and Chemicals

Europium(III) stock solution (10^{-4} mol/L) is obtained from the dissolution of Eu_2O_3 (Johnson Matthey, 99.99%) in $HClO_4$. All solutions are prepared using milli-Q water from a Direct Q3 Millipore. Suwannee river fulvic acid (2S101F) is purchased from the International Humic Substances Society and used as received. The ionic strength is fixed with $NaClO_4$ (Sigma Aldrich, >98%) at 0.02 M, 0.1 M and 0.5 M. The pH values are fixed at 4, 6, and 7 by the addition of small amounts of freshly prepared 0.1 M NaOH and/or $HClO_4$. Measurements are done using a pH meter Seven Easy (Mettler Toledo) with a combined glass electrode Inlab micro, filled with $NaClO_4$ 3M to avoid $KClO_4$ precipitation in the frit of the electrode with the original KCl filling. The electrode signal in mV is calibrated using commercial buffer solutions (pH 4.01, 7.01, and 10.00).

4.2. Time-Resolved Luminescence Spectroscopy

The experimental set-up and luminescence decay times fitting have already been described elsewhere.[5,24,26,28] The 600 lines.mm^{-1} grating of the Acton spectrometer (slit 1 mm) is used. The luminescence signal is collected during a gate width (*W*) of 300 μs, at a gate delay (*D*) of 10 μs after the excitation by the laser flash. To increase the signal to noise ratio, 1,000 to 10,000 accumulations are performed for each spectrum, the background noise is subtracted, and the luminescence is divided by the average of 100 laser shots energy before and after the acquisition, and by the number of acquisitions (accumulations).

Because of the weak energy received by the system during the experiments, photochemical reactions of humic substances[57] can be excluded. The excitation wavelength is set at λ_{exc} = 393.7 nm, with an energy typically less than 2 mJ, which corresponds to the $^5L_6 \leftarrow ^7F_0$ transition of Eu(III). After inner conversion, the observed luminescence corresponds to the transitions from the $^5D_0$ excited state to the ground ^7F_j manifold.[58] We focus our attention on three transitions: the $^5D_0 \rightarrow ^7F_0$ transition (λ_{max} = 578.8 nm), forbidden by the selection rules but apparent when Eu(III) chemical environment loses its centro-symmetry; the $^5D_0 \rightarrow ^7F_1$ transition (λ_{max} = 591.1 nm), a magnetic dipole transition; and the $^5D_0 \rightarrow ^7F_2$ electric dipole

transition (λ_{max} = 615.1 nm), which is very sensitive to europium speciation,[59] and known as a hypersensitive transition. The peak area ratio between the $^5D_0 \rightarrow {}^7F_2$ and the $^5D_0 \rightarrow {}^7F_1$ transitions, hereafter referred as the asymmetry ratio $^7F_2/^7F_1$, has often been used to estimate complexation constants,[60] and structural modifications.[5]

4.3. Modeling

Modeling of Eu-SRFA interactions is performed using ECOSAT software,[61] which includes speciation with inorganic ligands and humic substances through the NICA- Donnan model.[10] It merges the Non-Ideal Competitive Adsorption (NICA) model with a continuous distribution of sites, and a Donnan potential description to account for electrostatic interactions within the structure of HS considered as a water-permeable gel. The model accounts for electrostatic interactions,[62] sites heterogeneity, non-ideality of the metal-HS complexation, and competition between metals. Milne et al. proposed generic data for HA and FA complexation with protons,[33] and several metals of interest, including Ln(III) and An(III).[34] The inorganic side reactions of Eu(III) with OH^- are implemented in the ECOSAT database.[63]

Site densities of the two distribution of sites of SRFA—$Q_{max,1}$, and $Q_{max,2}$—, parameters representing the intrinsic heterogeneity—widths of the distributions of sites p_1 and p_2—, and generic proton parameters—non-ideality parameter $n_{H^+,i}$, and median affinity constant $log_{10}\tilde{K}_{H^+,i}$—for low-affinity type of sites—so-called carboxylic S_1—and high-affinity type of sites—so-called phenolic S_2—proposed by Milne et al.[33,34] are recalled in Table S1 of the Supporting Information (SI).

5. Results and discussion

5.1. Spectroscopic data

Eu(III) speciation is first studied at fixed pH values of 4, 6, and 7, fixed ionic strength of 0.1 M, and at varying $C_{Eu(III)}$—0.5, 1, and 10 µM—and SRFA concentrations —from 0 to 2,8 g_{SRFA}/L. The obtained luminescence spectra shown in Figure S1 of the SI are normalized to the peak area of the $^5D_0 \rightarrow {}^7F_1$ transition. The complexation of Eu(III) in the system is evidenced by the increase of both the forbidden $^5D_0 \rightarrow {}^7F_0$ and the hypersensitive $^5D_0 \rightarrow {}^7F_2$ transitions. The $^5D_0 \rightarrow {}^7F_0$ transition appears at pH above 5 in the absence of SRFA, or in the presence of a slight amount of SRFA at whatever pH value. This typically indicates a loss of

centro-symmetry compared to the aquo-complex $Eu(H_2O)_n^{3+}$ and the formation of $Eu(OH)_n^{(3-n)+}$—minor under these pH conditions—and Eu(III)-SRFA complexes.

The $^5D_0 \rightarrow {}^7F_2$ transition relative intensity is increasing with complexation[59]—here with SRFA concentration—and shows a narrowing with metal complexation and a shift toward lower wavelengths (see Figure S1 of the SI). The variation of the relative intensity of $^5D_0 \rightarrow {}^7F_2$ area to the $^5D_0 \rightarrow {}^7F_1$ area with C_{SRFA}, provides information on Eu(III) chemical environment. It is then possible to use this evolution as a spectral titration curve.[60]

The evolutions of the asymmetry ratio $^7F_2/{}^7F_1$ *vs.* C_{SRFA} at different pH values, $C_{Eu(III)}$ (Figure 1) are showing unusual features. Two different Eu(III) luminescence behaviors are evidenced. First, the peak area ratio shows an increase with C_{SRFA} values—C_{SRFA} < 100 mg_{SRFA}/L at pH 4, C_{SRFA} < 40 mg_{SRFA}/L at pH 6, and C_{SRFA} < 20 mg_{SRFA}/L at pH 7—until a plateau seems to be reached. This evolution reflects the typical luminescence evolution of Eu(III) complexed by organic compounds.[5,64-66] Second, after the plateau the asymmetry ratio keeps on increasing with C_{SRFA}. Chung et al.[21] reported a decrease in the asymmetry ratio after the plateau with increasing $C_{Eu(III)}$ in the case of a soil FA, but we interpret this evolution as the saturation of their humic extracts and the increase of the proportion of free Eu in the system.

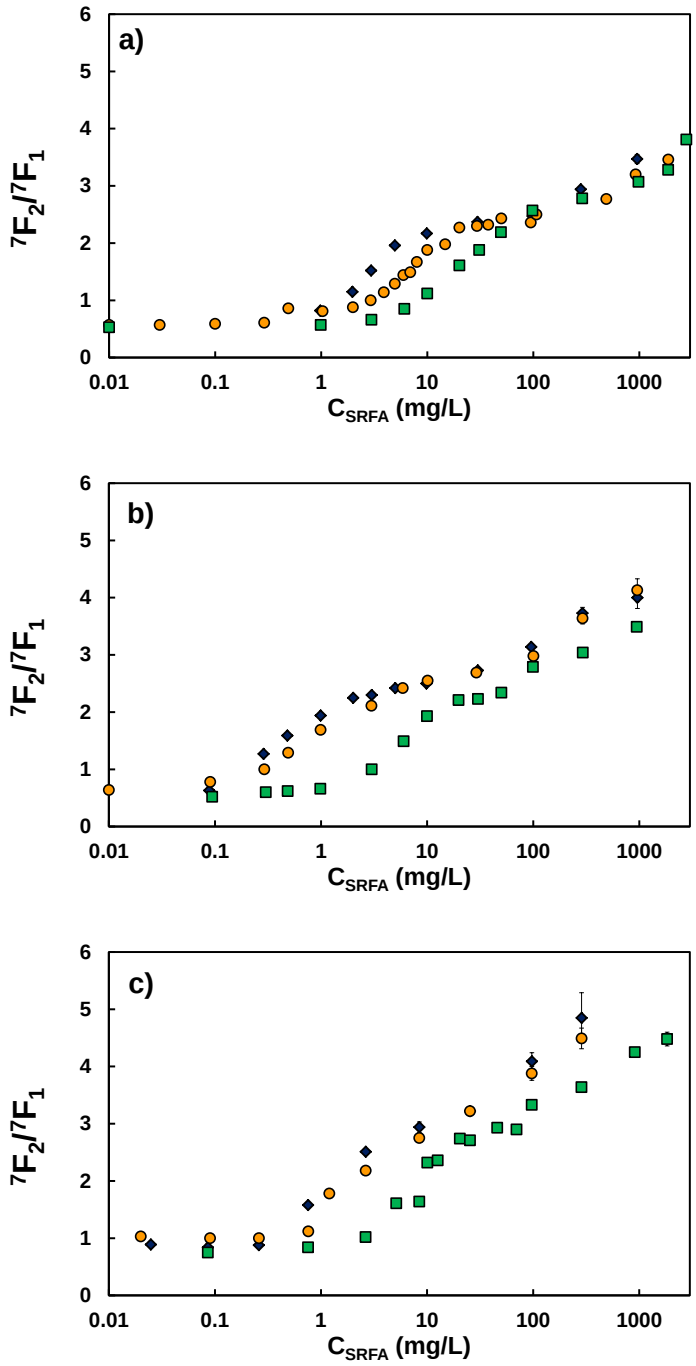

Figure 1. Evolution of $^5D_0 \rightarrow {}^7F_2/{}^5D_0 \rightarrow {}^7F_1$ area ratios *vs.* C_{SRFA} at I = 0.1 M, pH 4 (a); pH 6 (b), and pH 7 (c) for $C_{Eu(III)}$ of 0.5 (blue diamonds), 1 (orange circles), and 10 µM (green squares): λ_{exc} = 393.7 nm, D = 10 µs, W = 300 µs, 600 lines.mm^{-1} grating. Error bars represent 2σ of the area ratio using the trapezoid method.

5.2. Decay time evolutions

Eu(III) luminescence decay times were measured with an initial delay D = 10 µs, a gate step of 15 µs, and a gate width W = 300 µs for $C_{Eu(III)}$ of 1 µM and 10 µM at pH 4, 6 and 7 (Figure S2 of the SI)—the signal at $C_{Eu(III)}$ = 0.5 µM being too weak to obtain a reliable decay time analysis.

At pH 4 (Figure S2a of the SI), Eu(III) is showing a mono-exponential decay up 2.98 mg_{SRFA}/L. The τ values do not differ from the free Eu^{3+} one, *i.e.* τ = 110 µs.[12,13] For C_{SRFA} higher than 2.98 mg/L, bi-exponential decays are obtained, which could be attributed to the presence of two radiative decay processes linked to two different excited species.[26] The first decay τ_1 is faster than free Eu^{3+}, and does not seem to vary strongly with SRFA concentration.[5,28] The relationships that links the hydration number cannot be applied, as in the case of benzoic acids.[64,66-68] The second decay, τ_2, is slower than free Eu^{3+}, and is showing two different comportments as a function of $C_{Eu(III)}$. From 2.98 up to *ca.* 100 mg_{SRFA}/L—*i.e.*, the C_{SRFA} value where all the $^7F_1/^7F_2$ evolution are merging in Figure 1—, the τ_2 value is increasing up to *ca.* 180 µs whatever the $C_{Eu(III)}$. This is the typical comportment of Eu(III) complexed by HS, which can be interpreted as the substitution of inner-sphere water molecules by SRFA functionalities. The τ_2 value *ca.* 175 µs is in agreement with the evolution observed for Eu-HS complexes.[24] The application of the relationship from Kimura and Choppin[13] is debatable, but would indicate the loss of *ca.* 3.6 ± 0.5 water molecules. At higher C_{SRFA} values, the decay time evolutions are more intricate to interpret. If τ_2 values keep on increasing for $C_{Eu(III)}$ = 1 µM—*i.e.*, τ_2 *ca.* 235 µs and a loss of *ca.* 5.2 ± 0.5 water molecules— they also seem to attain a plateau. Conversely, τ_2 seems to decrease for $C_{Eu(III)}$ = 10 µM. The application of the relationship from Kimura and Choppin[13] has no sense here as it would indicate a "gain" of *ca.* 1.4 ± 0.5 water molecules between 100 and 1000 mg_{SRFA}/L, when the increases in both $^5D_0 \rightarrow ^7F_0$ area and asymmetry ratio (Figure 1) indicate a continuing change in the complexation environment of Eu(III). The combination of the apparent plateau for $C_{Eu(III)}$ = 1 µM and the decrease at 10 µM, may lead to a possible dynamic quenching, the origin of which is not possible to determine and would require further investigations.

At pH 6 (Figure S2b of the SI), only mono-exponential decays can be fitted for C_{SRFA} lower than 30 mg/L There is only a very slight increase in the τ values from *ca.* 100 to *ca.* 140 µs—loss of *ca.* 2.2 ± 0.5 water molecules. Bi-exponential decays are obtained for C_{SRFA} higher than 30 mg_{SRFA}/L for $C_{Eu(III)}$ of 1 and 10 µM up to 1 g_{SRFA}/L. One also note the difference

between $C_{Eu(III)}$, which is reminiscent of the evolution at pH 4 and would also indicate a quenching mechanism. The final situation at $C_{Eu(III)}$ and C_{SRFA} = 1 g_{SRFA}/L would indicate the loss of *ca.* 5.8 ± 0.5 water molecules.

At pH 7 (Figure S2c of the SI), mono-exponential decays are first obtained at lower C_{SRFA}. Bi-exponential decays are obtained for C_{SRFA} higher than 3 mg_{SRFA}/L for $C_{Eu(III)}$ of 1 and 10 µM. The obtained decays are showing a slight increase in τ_1 and a stronger continuous increase in τ_2 up to 285 µs for $C_{Eu(III)}$ = 10 µM—loss of *ca.* 6.0 ± 0.5 water molecules. Both Eu(III) concentration seem to follow the same trend even if the τ_2 value for $C_{Eu(III)}$ = 10 µM and C_{SRFA} = 1 g_{SRFA}/L is clearly below the trend. The possible quenching mechanism seems to be less operant here.

Nevertheless, the decay time evolutions seem to confirm that different environments are present at different C_{SRFA}. The estimation of hydration sphere here is constrained by the relationship from Kimura and Choppin[13], the validity of which has not been demonstrated up to now in these systems.

5.3. Effect of ionic strength

In order to improve the understanding of the second mode in the complexation isotherms, we performed experiments at pH 7 and various ionic strengths (I = 0.02, 0.1, and 0.5 M $NaClO_4$), which asymmetry ratios' evolutions are shown in Figure 2. First, before the plateau, *i.e.*, < 10 mg_{SRFA}/L, the complexation is decreasing as expected with ionic strength,[10,69] whilst a reverse influence is shown at higher C_{SRFA}. This second part, where the peak area ratio is still increasing, means that the chemical environment of Eu(III) is ionic strength dependent. If one considers that the decrease of the asymmetry ratio with ionic strength at low C_{SRFA} indicates a typical weaker binding,[18,69,70] then one can also consider that the increase in asymmetry ratio at higher C_{SRFA} with ionic strength indicates a stronger binding environment. This was never reported in previous studies focusing on metal-organic matter speciation.[24]

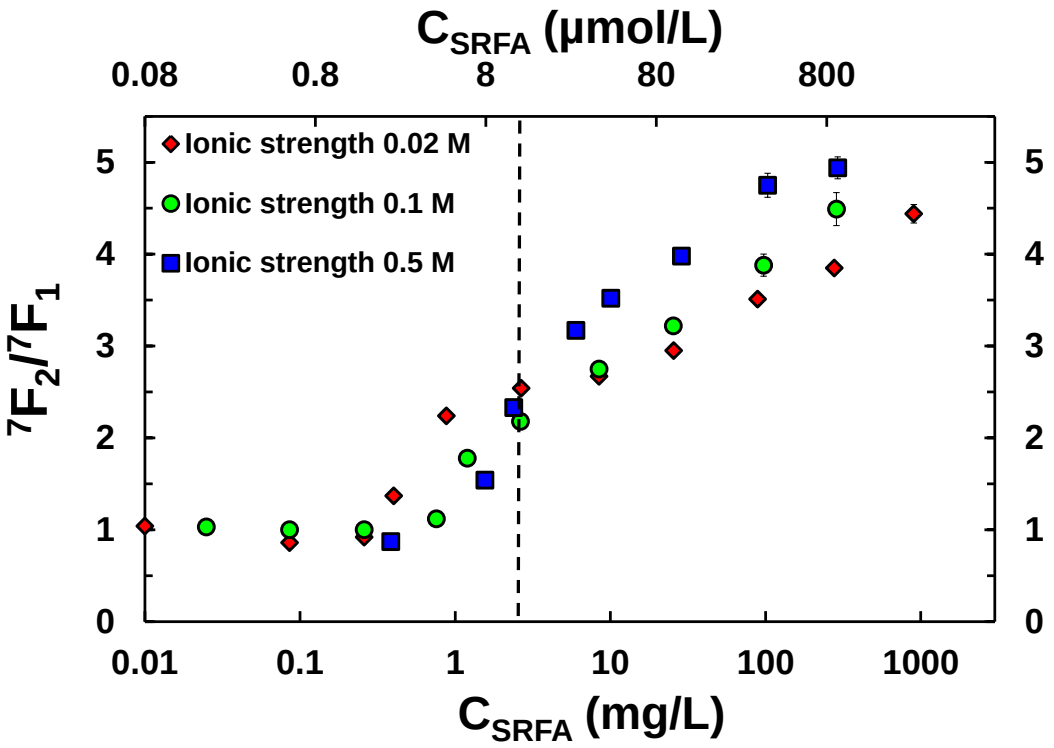

Figure 2. Evolution of $^5D_0 \rightarrow {}^7F_2/{}^5D_0 \rightarrow {}^7F_1$ area ratios *vs.* C_{SRFA} the ionic strength (I = 0.02 M, red diamonds; I = 0.1 M, green circles; I = 0.5 M, blue squares) at $C_{Eu(III)}$ of 1 µM and pH 7. Dashed line corresponds to the inversion of the ionic strength trend.

5.4. Simulation and modeling

For a better understanding of the second mode in complexation isotherms, simulations of Eu(III)-SRFA complexation are done using NICA-Donnan generic parameters[34] for $C_{Eu(III)}$ of 0.5, 1 and 10 µM, at I = 0.1 M (Figure S3 of the SI). Eu(III) is increasingly fixed to SRFA, mostly to S_1 sites at pH 4. The proportion of Eu(III) bound to S_2 sites is increasing with pH. The total complexation is expected around C_{SRFA}= 100 mg_{SRFA}/L for pH 4, C_{SRFA} = 40 mg_{SRFA}/L for pH 6, and C_{SRFA} = 20 mg_{SRFA}/L for pH 7. No account for mixed $Eu(OH)_nFA$ complexes is needed in these simulations *vs.* pH. Nevertheless, it can be recalled that mixed Fe(OH)HA, and Al(OH)HA complexes was proposed in the framework of NICA-Donnan[40] or Model VI,[39] respectively. No further modification of the speciation is expected from the calculation at higher C_{SRFA}. Therefore, the further increase of asymmetry ratio should correspond to another complexation/fixation mode not accounted for by any available model, yet.

It is then possible to compare our dataset to the prediction of the NICA-Donnan model. First, the asymmetry ratios are used as indicators of the proportion of Eu(III) complexed to SRFA

(Figure S4 of the SI).[60] The asymmetry ratio evolves with the metal to SRFA concentration ratio. When SRFA is not present in the system, the asymmetry ratio is the one for the Eu(III) aquo-complex. When the asymmetry ratio is reaching a plateau at pH 4 (Figure S4 of the SI), this suggests that all of Eu(III) is complexed to SRFA. This evolution is used as a spectral titration curve to calculate proportions of Eu(III) bound to SRFA (Figure 3a).[60] At pH 6, the existence of a plateau is less clear (Figure 1b) but seems to occur for C_{SRFA} of 10 mg_{SRFA}/L for $C_{Eu(III)}$ of 0.5 µM and 1 µM, and for C_{SRFA} of 30 mg_{SRFA}/L for $C_{Eu(III)}$ of 10 µM. These values are supported by our previous simulations (*vide supra*, Figure S3 of the SI). At pH 6, Eu(III) is totally bound to the SRFA for concentrations *ca.* 10 mg_{SRFA}/L for $C_{Eu(III)}$ of 0.5 µM, and 1 µM, and for concentration *ca.* 30 mg_{SRFA}/L for $C_{Eu(III)}$ of 10 µM. At pH 7 (Figure 1c), the end of the first complexation mode is set as for pH 6, when Eu(III) is fully bound to SRFA in our previous simulations, for concentrations of 2.6 mg_{SRFA}/L for $C_{Eu(III)}$ of 0.5 and 1 µM and 10 mg_{SRFA}/L for $C_{Eu(III)}$ of 10 µM.

For a better fit, NICA-Donnan parameters for Eu(III)-SRFA binding are adjusted. The adjustment of Eu(III) binding parameters for S_1 sites is done at pH 4 only, because at higher pH values, due the presence of hydrolyzed species of Eu(III), the asymmetry ratio at low SFRA concentration could not correspond to free Eu^{3+}. Thus, the adjusted parameters for the low proton affinity sites S_1 at pH 4 are used at pH 6 and 7 to adjust the parameters for the high proton affinity sites S_2.

The proportion of Eu(III)-SRFA complex for $C_{Eu(III)}$ of 0.5, 1, and 10 µM at pH 4, 6, and 7, and the modeling of Eu(III) bound to SRFA are shown in Figure 3. NICA-Donnan parameters for proton and Eu(III) binding to SRFA used in the model are presented in Table S1 of the SI. The model is slightly underestimating the complexation for $C_{Eu(III)}$ = 0.5 µM at pH 4, but it is still in fair agreement with experimental data. It is worthy to notice in Table S1 of the SI that compared to generic parameters, Eu(III) complexation by SRFA is less important—lower $\log_{10}\tilde{K}_{Eu^{3+},1}$— and the distribution is more heterogeneous for S_1 sites—lower $n_{Eu^{3+},1}$—, and that the complexation is stronger and less heterogeneous for S_2 sites—higher $\log_{10}\tilde{K}_{Eu^{3+},2}$, and higher $n_{Eu^{3+},2}$. Milne et al.[34] proposed correlation between $n_{M^{n+},i}$ and $n_{M^{n+},i}\times\log_{10}\tilde{K}_{M^{n+},i}$ *vs.* $\log_{10}{}^{*}\beta^{\circ}_{1}$. As it can be anticipated from the very little difference between the simulations using generic parameters[34] and the modeling of our data, it can be seen in Table S1 of the SI that $n_{Eu^{3+},1}\times\log_{10}\tilde{K}_{Eu^{3+},1}$ are in good agreement. Nevertheless, it seems that $n_{Eu^{3+},2}\times\log_{10}\tilde{K}_{Eu^{3+},2}$ is higher in our case leading to a slightly higher complexation than anticipated.

In the NICA-Donnan model, the ratio between the non-ideality parameter for metal and proton ($n_{M^{n+},i}/n_{H^+,i}$) for each type of sites gives information on the number of protons expelled for each metal bound to HS, and thus to stoichiometry. The values of $n_{Eu^{3+},1}/n_{H^+,1}$ = 0.80 and $n_{Eu^{3+},2}/n_{H^+,2}$ = 0.52 suggest that europium is mostly bound in monodentate and bidentate form, respectively, as it was previously seen for a sedimentary humic acid extract.[23]

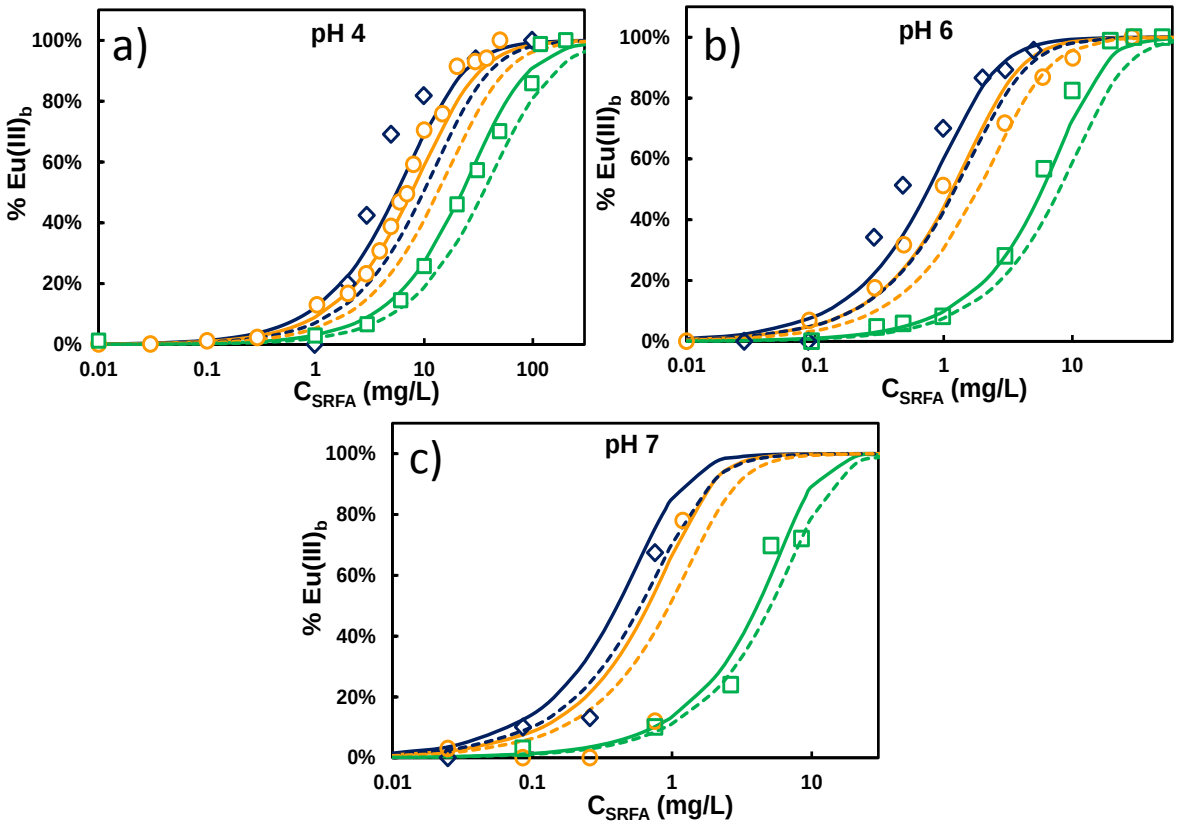

Figure 3. Proportion of Eu(III) bound to SRFA for Eu(III) concentrations of 0.5 µM (blue diamonds), 1 µM (orange circles) and 10 µM (green squares) at pH 4 (a), 6 (b), and 7 (c). The dashed lines are the simulations and the solid lines are the results of our modeling of Eu(III) bound to SRFA. Adjusted and generic NICA Donnan parameters are given in Table S1 of the SI.

5.5. Eu(III)-SRFA interactions

It was possible to satisfactorily describe Eu(III)-SRFA interactions that occur in the first parts of the isotherms with the NICA-Donnan model. The increase in asymmetry ratio at higher C_{SRFA} with ionic strength (Figure 2), which indicates a change in the complexation environment, still needs to be cleared. The influence of varying metal concentration with constant HS concentration—see Hummel et al.[70] and references therein—is directly accounted for within the NICA-Donnan model,[71] and is not in play here. Assumptions are made, which

may not necessarily exclude each other, regarding this original asymmetry ratio evolution at the higher C_{SRFA}: (i) it may correspond to the formation of another type of complex, *e.g.*, strong sites *vs.* weak sites or a 1:2 complex[72-74]; (ii) and/or it can reflect a different spatial organization of the complexed europium constrained by a change in the SRFA structure. As the UV-Visible absorption of HS decreases rather monotonously with wavelength, one may also propose higher auto absorption of the $^5D_0 \rightarrow {}^7F_1$ transition wavelength span compared to the $^5D_0 \rightarrow {}^7F_2$ transition one with C_{SRFA}. The fact that the second increase occurs at lower C_{SRFA} with pH permits to exclude this hypothesis.

A possible explanation may rely in the influence of ionic strength on complexation and adsorption. Following the Debye-Hückel theory, the decrease in complexation with ionic strength at low C_{SRFA} is in line with the evolution of the activity coefficient with the reciprocal of the Debye length (κ).[75] This indicates that at low C_{SRFA} the complexation occurs with rather isolated functional groups in the SRFA structure. At higher C_{SRFA} one can consider the interaction between SRFA entities as supramolecular associations of fulvic acid particles.[47,49] The variation of the hydrodynamic radius (R_H) with ionic strength of the smallest entities of HS, including SRFA, has given contrasted results.[76,77] When d'Orlyé and Reiller[77] did not evidence a clear increase in R_H with ionic strength at pH 10 in Taylor dispersion analysis, Domingos et al.[76] reported a small decrease of diffusion coefficient of SRFA—small increase in R_H—with ionic strength between pH 2 and 8 in fluorescence correlation spectroscopy. This latter result was interpreted as a reduction of both intramolecular and intermolecular repulsion. Decreasing intramolecular repulsion will lead to molecular compression, while decreasing intermolecular repulsion can increase aggregation. It has also been shown that contrary to simple organics—and commonly to polyelectrolytes[78,79]—, adsorption of humic substances onto minerals is increasing with ionic strength.[5,80] Even if this effect is much weaker for FA compared to HA,[81] this means that HS entities in general can approach at shorter distances to each other in solution with increasing ionic strength. Following the Gouy-Chapman theory, Eu(III)-bearing SRFA entities can more easily approach each other with increasing ionic strength. The second part of the asymmetry ratio increase could therefore be due to the formation of complexes with higher stoichiometry between complexation sites that are not located on the same HS entity or "particle". This suggests that there might be electrostatic driven interactions between fulvic acid sites in particles that are typically complexing Eu(III)—intra-particulate complexation mode—, and form Eu(III)-bridged complexes in the second part of the asymmetry ratio evolution—inter-

particulate complexation mode. We can also notice that in complexation isotherms at pH 7 and various ionic strengths (Figure 2) the metal to ionized FA sites concentration ratio equals 10 at the boundary between the two-luminescence modes. In the second mode, we can assume that Eu(III)-bridged complexes are formed because of the decreasing metal to ionized FA sites concentration ratio.

The formation of 1:2 stoichiometry complexes was suggested by Bertha and Choppin[73] who studied interactions of HS (HA and FA) with Eu(III) and Am(III). Their results, using Schubert's method to determine binding constants, suggest the formation of 1:1 and 1:2 Eu-HS complexes from slope analyses of the variation of the distribution coefficient with humic acid concentration. At pH 4.5 Bertha and Choppin[73] proposed that Eu(III) is bound simultaneously by one or two carboxylate groups. In our study we could interpret our spectroscopically observed evolutions as the successive formation of the 1:1 and 1:2 Eu(III)-SRFA complexes. The ionic strength effect in complexation isotherms suggests that complexation sites may not be located on the same fulvic acid particle. Such interactions are not yet accounted for in any model describing metal-HS interactions, and would require either complete rewriting of the models, or adaptation of the existing models to this not yet noticed effect.

Within the NICA-Donnan model framework, the Donnan volume V_D is optimized to build the acid-base titration master curves. It decreases with ionic strength following an empirical relationship.[62] The Donnan potential ψ_D inside this volume is assumed negative and constant inside, and nil outside the particle—or water-permeable Donnan gel. It can be calculated from the ratio of the activity of ions inside and outside the Donnan gel, and from the charge density inside the gel, so that the decrease in complexation with ionic strength is linked to a decrease in the negative value of q/V_D and ψ_D.[10] One could then think that the increase of Eu(III) association at high C_{SRFA} with ionic strength could be linked to an apparent increase in the negative value q/V_D and ψ_D. The verification of this hypothesis implies the determination of the size of Eu(III)-SRFA complexes at varying pH, Eu and SRFA concentrations, and ionic strength. It is nevertheless, worthy to recall that, as already discussed in Benedetti *et al.*,[62] the Donnan model seems not to be very realistic for FA because the changes in Donnan volumes as a function of ionic strength are too large.

Another possibility is the account of an interfacial potential, as a double layer spreading outside the Donnan gel as proposed by Saito et al.,[82,83] which should be implemented to be

effective at high C_{SRFA} and should mostly be ineffective at low C_{SRFA} in order to represent the already successful modeling obtained up to now within the framework of NICA-Donnan.

ASSOCIATED CONTENT

Supporting Information

The supporting information contains four Figures and one Table. One Figure shows Eu(III)-SRFA normalized luminescence spectra to the $^5D_0 \rightarrow {}^7F_1$ transition at 0.1 M $NaClO_4$ and C_{Eu}(III) = 1 µM at pH 4, 6 and 7. One Figure shows luminescence decay times of Eu(III) at pH 4, 6 and 7 depending on fulvic concentration for Eu(III) concentrations of 1 µM and 10 µM. One Figure shows the simulation of Eu bound to SRFA and NICA-Donnan parameters using generic parameters. One Figure shows the transformation of asymmetry ration in proportion of Eu(III) bound to the fulvic acid. One Table is showing the NICA-Donnan generic parameters for simulation, and the NICA-Donnan parameters obtained from modeling. This material is available free of charge via the Internet at http://pubs.acs.org.

ACKNOWLEDGMENT

Pr. Jose Paulo Pinheiro and Dr. Rute Domingos are acknowledged for useful conversations and suggestions. This work was partly financed by the inner RCHIM project within the RSTB program from CEA.

6. References

1. Binnemans, K.; Jones, P. T.; Blanpain, B.; van Gerven, T.; Yang, Y. X.; Walton, A.; Buchert, M. Recycling of rare earths: a critical review. *J. Clean. Prod.* **2013,** *51*, 1-22; DOI 10.1016/j.jclepro.2012.12.037.

2. McCarthy, J. F.; Czerwinski, K. R.; Sanford, W. E.; Jardine, P. M.; Marsh, J. D. Mobilization of transuranic radionuclides from disposal trenches by natural organic matter. *J. Contam. Hydrol.* **1998,** *30* (1-2), 49-77; DOI 10.1016/S0169-7722(97)00032-6.

3. McCarthy, J. F.; Sanford, W. E.; Stafford, P. L. Lanthanide field tracers demonstrate enhanced transport of transuranic radionuclides by natural organic matter. *Environ. Sci. Technol.* **1998,** *32* (24), 3901-3906; DOI 10.1021/es971004f.

4. Bryan, N. D.; Abrahamsen, L.; Evans, N.; Warwick, P.; Buckau, G.; Weng, L. P.; van Riemsdijk, W. H. The effects of humic substances on the transport of radionuclides: recent improvements in the prediction of behaviour and the understanding of mechanisms. *Appl. Geochem.* **2012,** *27* (2), 378-389; DOI 10.1016/j.apgeochem.2011.09.008.

5. Janot, N.; Benedetti, M. F.; Reiller, P. E. Influence of solution parameters on europium(III), α-Al_2O_3, and humic acid interactions: macroscopic and time-resolved laser-induced luminescence data. *Geochim. Cosmochim. Acta* **2013,** *123*, 35-54; DOI 10.1016/j.gca.2013.08.038.

6. Jones, M. N.; Bryan, N. D. Colloidal properties of humic substances. *Adv. Colloid Interface Sci.* **1998,** *78* (1), 1-48; DOI 10.1016/S0001-8686(98)00058-X.

7. Hummel, W., Binding models for humic substances. In *Modelling in Aquatic Chemistry*, Grenthe, I.; Puigdomènech, I., Eds. OECD's Nuclear Energy Agency: Paris, France, 1997; pp 153-206.

8. Tipping, E. Humic ion-binding model VI: an improved description of the interactions of protons and metal ions with humic substances. *Aquat. Geochem.* **1998,** *4* (1), 3-48; DOI 10.1023/A:1009627214459.

9. Tipping, E.; Lofts, S.; Sonke, J. E. Humic ion-binding Model VII: a revised parameterisation of cation-binding by humic substances. *Environ. Chem.* **2011,** *8* (3), 225-235; DOI 10.1071/EN11016.

10. Kinniburgh, D. G.; van Riemsdijk, W. H.; Koopal, L. K.; Borkovec, M.; Benedetti, M. F.; Avena, M. J. Ion binding to natural organic matter: competition, heterogeneity, stoichiometry and thermodynamic consistency. *Colloids Surf. A* **1999,** *151* (1-2), 147-166; DOI 10.1016/S0927-7757(98)00637-2.

11. Bünzli, J.-C. G., Luminescent probes. In *Lanthanides Probe in Life, Chemical and Earth Sciences - Theory and Practice*, Bünzli, J.-C. G.; Choppin, G. R., Eds. Elsevier: Amsterdam, The Netherlands, 1989; pp 219-293.

12. Horrocks, W. D., Jr.; Sudnick, D. R. Lanthanide ion probes of structure in biology. Laser-induced luminescence decay constants provide a direct measure of the number of metal-coordinated water-molecules. *J. Am. Chem. Soc.* **1979,** *101* (2), 334-340; DOI 10.1021/ja00496a010.

13. Kimura, T.; Choppin, G. R. Luminescence study on determination of the hydration number of Cm(III). *J. Alloys Compd.* **1994,** *213-214*, 313-317; DOI 10.1016/0925-8388(94)90921-0.

14. Bidoglio, G.; Grenthe, I.; Qi, P.; Robouch, P.; Omenetto, N. Complexation of Eu and Tb with fulvic acids as studied by time-resolved laser-induced fluorescence. *Talanta* **1991,** *38* (9), 999-1008; DOI 10.1016/0039-9140(91)80316-R.

15. Moulin, C.; Decambox, P.; Mauchien, P.; Moulin, V.; Theyssier, M. On the use of laser-induced time-resolved spectrofluorometry for interaction studies between organic matter and actinides: application to curium. *Radiochim. Acta* **1991,** *52-53*, 119-125; DOI 10.1524/ract.1991.5253.1.119.

16. Kim, J. I.; Wimmer, H.; Klenze, R. A study of curium(III) humate complexation by time resolved laser induced fluorescence spectroscopy (TRLFS). *Radiochim. Acta* **1991,** *54* (1), 35-41; DOI 10.1524/ract.1991.54.1.35.

17. Yoon, T. H.; Moon, H.; Park, Y. J.; Park, K. K. Investigation of metal binding sites on soil fulvic acid using Eu(III) luminescence spectroscopy. *Environ. Sci. Technol.* **1994,** *28* (12), 2139-2146; DOI 10.1021/es00061a023.

18. Czerwinski, K. R.; Kim, J. I.; Rhee, D. S.; Buckau, G. Complexation of trivalent actinides ions (Am^{3+}, Cm^{3+}) with humic acids: the effect of ionic strength. *Radiochim. Acta* **1996,** *72* (4), 179-187; DOI 10.1524/ract.1996.72.4.179.

19. Moulin, C.; Wei, J.; van Iseghem, P.; Laszak, I.; Plancque, G.; Moulin, V. Europium complexes investigations in natural waters by time-resolved laser-induced fluorescence. *Anal. Chim. Acta* **1999,** *396* (2-3), 253-261; DOI 10.1016/S0003-2670(99)00427-4.

20. Morgenstern, M.; Klenze, R.; Kim, J. I. The formation of mixed-hydroxo complexes of Cm(III) and Am(III) with humic acid in the neutral pH range. *Radiochim. Acta* **2000,** *88* (1), 7-16; DOI 10.1524/ract.2000.88.1.007.

21. Chung, K. H.; Lee, W.; Cho, Y.; Choi, G. S.; Lee, C. W. Comparison of synchronous and laser-induced fluorescence spectroscopy applied to the Eu(III)-fulvate complexation. *Talanta* **2005,** *65* (2), 389-395; DOI 10.1016/j.talanta.2004.06.026.

22. Kumke, M. U.; Eidner, S.; Kruger, T. Fluorescence quenching and luminescence sensitization in complexes of Tb^{3+} and Eu^{3+} with humic substances. *Environ. Sci. Technol.* **2005,** *39* (24), 9528-9533; DOI 10.1021/es051437f.

23. Marang, L.; Reiller, P. E.; Eidner, S.; Kumke, M. U.; Benedetti, M. F. Combining spectroscopic and potentiometric approaches to characterize competitive binding to humic substances. *Environ. Sci. Technol.* **2008,** *42* (14), 5094-5098; DOI 10.1021/es702858p.

24. Brevet, J.; Claret, F.; Reiller, P. E. Spectral and temporal luminescent properties of Eu(III) in humic substance solutions from different origins. *Spectrochim. Acta, Part. A* **2009,** *74* (2), 446-453; DOI 10.1016/j.saa.2009.06.042.

25. Marang, L.; Eidner, S.; Kumke, M. U.; Benedetti, M. F.; Reiller, P. E. Spectroscopic characterization of the competitive binding of Eu(III), Ca(II), and Cu(II) to a sedimentary originated humic acid. *Chem. Geol.* **2009,** *264* (1-4), 154-161; DOI 10.1016/j.chemgeo.2009.03.003.

26. Reiller, P. E.; Brevet, J. Bi-exponential decay of Eu(III) complexed by Suwannee River humic substances: spectroscopic evidence of two different excited species. *Spectrochim. Acta, Part. A* **2010,** *75* (2), 629-636; DOI 10.1016/j.saa.2009.11.029.

27. Lukman, S.; Saito, T.; Aoyagi, N.; Kimura, T.; Nagasaki, S. Speciation of Eu^{3+} bound to humic substances by time-resolved laser fluorescence spectroscopy (TRLFS) and parallel factor analysis (PARAFAC). *Geochim. Cosmochim. Acta* **2012,** *88*, 199-215; DOI 10.1016/j.gca.2012.04.023.

28. Janot, N.; Benedetti, M. F.; Reiller, P. E. Colloidal α-Al_2O_3, europium(III) and humic substances interactions: a macroscopic and spectroscopic study. *Environ. Sci. Technol.* **2011,** *45* (8), 3224-3230; DOI 10.1021/Es102592a.

29. Sonke, J. E.; Salters, V. J. M. Lanthanide-humic substances complexation. I. Experimental evidence for a lanthanide contraction effect. *Geochim. Cosmochim. Acta* **2006,** *70* (6), 1495-1506; DOI 10.1016/j.gca.2005.11.017.

30. Sonke, J. E. Lanthanide-humic substances complexation. II. Calibration of humic ion-binding Model V. *Environ. Sci. Technol.* **2006,** *40* (24), 7481-7487; DOI 10.1021/es060490g.

31. Pourret, O.; Davranche, M.; Gruau, G.; Dia, A. Rare earth elements complexation with humic acid. *Chem. Geol.* **2007,** *243* (1-2), 128-141; DOI 10.1016/j.chemgeo.2007.05.018.

32. Pearson, R. G. Hard and soft acids and bases. *J. Am. Chem. Soc.* **1963,** *85* (22), 3533-3539; DOI 10.1021/ja00905a001.

33. Milne, C. J.; Kinniburgh, D. G.; Tipping, E. Generic NICA-Donnan model parameters for proton binding by humic substances. *Environ. Sci. Technol.* **2001,** *35* (10), 2049-2059; DOI 10.1021/es000123j

34. Milne, C. J.; Kinniburgh, D. G.; van Riemsdijk, W. H.; Tipping, E. Generic NICA-Donnan model parameters for metal-ion binding by humic substances. *Environ. Sci. Technol.* **2003,** *37* (5), 958-971; DOI 10.1021/es0258879.

35. Guillaumont, R.; Fanghänel, T.; Fuger, J.; Grenthe, I.; Neck, V.; Palmer, D. A.; Rand, M., *Chemical Thermodynamics 5. Update on the Chemical Thermodynamics of Uranium, Neptunium, Plutonium, Americium and Technetium*. North Holland Elsevier Science Publishers B. V.: Amsterdam, The Netherlands, 2003; Vol. 5, p 918.

36. Dierckx, A.; Maes, A.; Vancluysen, J. Mixed complex formation of Eu^{3+} with humic acid and a competing ligand. *Radiochim. Acta* **1994,** *66/67*, 149-156; DOI 10.1524/ract.1994.6667.special-issue.149.

37. Glaus, M. A.; Hummel, W.; van Loon, L. R. Stability of mixed-ligand complexes of metal ions with humic substances and low molecular weight ligands. *Environ. Sci. Technol.* **1995,** *29* (8), 2150-2153; DOI 10.1021/es00008a039.

38. Panak, P.; Klenze, R.; Kim, J. I. A study of ternary complexes of Cm(III) with humic acid and hydroxide or carbonate in neutral pH range by time resolved laser fluorescence spectroscopy. *Radiochim. Acta* **1996,** *74* (Issue s1), 141-146; DOI 10.1524/ract.1996.74.special-issue.141.

39. Tipping, E.; Rey-Castro, C.; Bryan, S. E.; Hamilton-Taylor, J. Al(III) and Fe(III) binding by humic substances in freshwaters, and implications for trace metal speciation. *Geochim. Cosmochim. Acta* **2002,** *66* (18), 3211-3224; DOI 10.1016/S0016-7037(02)00930-4.

40. Weber, T.; Allard, T.; Tipping, E.; Benedetti, M. F. Modeling iron binding to organic matter. *Environ. Sci. Technol.* **2006,** *40* (24), 7488-7493; DOI 10.1021/es0607077.

41. Janot, N.; Reiller, P. E.; Benedetti, M. F. Modelling Eu(III) speciation in a Eu(III)/humic acid/α-Al_2O_3 ternary system. *Colloids Surf. A* **2013,** *435*, 9-15; DOI 10.1016/j.colsurfa.2013.02.052.

42. Pourret, O.; Davranche, M.; Gruau, G.; Dia, A. Competition between humic acid and carbonates for rare earth elements complexation. *J. Colloid Interface Sci.* **2007,** *305* (1), 25-31; DOI 10.1016/j.jcis.2006.09.020.

43. Stockdale, A.; Bryan, N. D. Uranyl binding to humic acid under conditions relevant to cementitious geological disposal of radioactive wastes. *Miner. Mag.* **2012,** *76* (8), 3391-3399; DOI 10.1180/minmag.2012.076.8.52.

44. Stockdale, A.; Bryan, N. D.; Lofts, S.; Tipping, E. Investigating humic substances interactions with Th^{4+}, UO_2^{2+}, and NpO_2^{+} at high pH: relevance to cementitious disposal of radioactive wastes. *Geochim. Cosmochim. Acta* **2013,** *121*, 214-228; DOI 10.1016/j.gca.2013.07.009.

45. Belfiore, L. A.; McCurdie, M. P.; Ueda, E. Polymeric coordination complexes based on cobalt, nickel, and ruthenium that exhibit synergistic thermal properties. *Macromolecules* **1993,** *26* (25), 6908-6917; DOI 10.1021/ma00077a031.

46. Wieder, R. K. Metal cation binding to *sphagnum* peat and sawdust: relation to wetland treatment of metal-polluted waters. *Water, Air, Soil Pollut.* **1990,** *53* (3-4), 391-400; DOI 10.1007/BF00170751.

47. Piccolo, A. The supramolecular structure of humic substances: a novel understanding of humus chemistry and implications in soil science. *Adv. Agron.* **2002,** *75*, 57-134; DOI 10.1016/S0065-2113(02)75003-7.

48. Schaumann, G. E.; Lang, F.; Frank, J. *Do multivalent cations induce cross-links in DOM precipitates?* In Humic Substances-Linking Structure to Functions, Proceedings of the 13th Meeting of the International Humic Substances Society. Universität Karlsruhe, Karlsruhe, Germany. July 30 - August 4, 2006; pp 941-944.

49. Kunhi Mouvenchery, Y.; Kučerík, J.; Diehl, D.; Schaumann, G. E. Cation-mediated cross-linking in natural organic matter: a review. *Rev. Environ. Sci Biotechnol.* **2012,** *11* (1), 41-54; DOI 10.1007/s11157-011-9258-3.

50. Engebretson, R. R.; von Wandruszka, R. The effect of molecular size on humic acid associations. *Org. Geochem.* **1997,** *26* (11), 759-767; DOI 10.1016/S0146-6380(97)00057-0.

51. Engebretson, R. R.; von Wandruszka, R. Kinetic aspects of cation-enhanced aggregation in aqueous humic acids. *Environ. Sci. Technol.* **1998,** *32* (4), 488-493; DOI 10.1021/es970693s.

52. von Wandruszka, R.; Engebretson, R. R., Kinetics of humic acid associations. In *Humic Substances and Chemical Contaminants*, Clapp, C. E.; Hayes, M. H. B.; Senesi, N.; Bloom, P. R.; Jardine, P. M., Eds. Soil Science Society of America: Madison, WI, USA, 2001; pp 119-126.

53. Plaschke, M.; Rothe, J.; Schäfer, T.; Denecke, M. A.; Dardenne, K.; Pompe, S.; Heise, K. H. Combined AFM and STXM in situ study of the influence of Eu(III) on the agglomeration of humic acid. *Colloids Surf. A* **2002,** *197* (1-3), 245-256; DOI 10.1016/S0927-7757(01)00901-3.

54. Plaschke, M.; Rothe, J.; Denecke, M. A.; Fanghänel, T. Soft X-ray spectromicroscopy of humic acid europium(III) complexation by comparison to model substances. *J. Electron. Spectrosc. Rel. Phenom.* **2004,** *135* (1), 53-62; DOI 10.1016/j.elspec.2003.12.007.

55. Naber, A.; Plaschke, M.; Rothe, J.; Hofmann, H.; Fanghänel, T. Scanning transmission X-ray and laser scanning luminescence microscopy of the carboxyl group and Eu(III) distribution in humic acid aggregates. *J. Electron. Spectrosc. Rel. Phenom.* **2006,** *153* (3), 71-74; DOI 10.1016/j.elspec.2006.06.005.

56. MacCarthy, P. The principles of humic substances. *Soil Sci.* **2001,** *166* (11), 738-751; DOI 10.1097/00010694-200111000-00003.

57. Monsallier, J.-M.; Scherbaum, F. J.; Buckau, G.; Kim, J.-I.; Kumke, M. U.; Specht, C. H.; Frimmel, F. H. Influence of photochemical reactions on the complexation of humic acid

with europium (III). *J. Photochem. Photobiol. A: Chem.* **2001,** *138* (1), 55-63; DOI S1010-6030(00)00380-4.

58. Carnall, W. T.; Fields, P. R.; Rajnak, K. Electronic energy levels of the trivalent lanthanide aquo ions. IV. Eu^{3+}. *J. Chem. Phys.* **1968,** *49* (10), 4450-4455; DOI 10.1063/1.1669896.

59. Jørgensen, C. K.; Judd, B. R. Hypersensitive pseudoquadrupole transitions in lanthanides. *Mol. Phys.* **1964,** *8* (3), 281-290; DOI 10.1080/00268976400100321.

60. Dobbs, J. C.; Susetyo, W.; Knight, F. E.; Castles, M. A.; Carreira, L. A.; Azarraga, L. V. A novel-approach to metal-humic complexation studies by lanthanide ion probe spectroscopy. *Int. J. Environ. Anal. Chem.* **1989,** *37* (1), 1-17; DOI 10.1080/03067318908026880.

61. Keizer, M. G.; van Riemsdijk, W. H. *A Computer Program for the Calculation of Chemical Speciation and Transport in Soil-Water Systems (ECOSAT 4.7)*; Wageningen Agricultural University: Wageningen, The Netherlands, 1994.

62. Benedetti, M. F.; van Riemsdijk, W. H.; Koopal, L. K. Humic substances considered as a heterogeneous Donnan gel phase. *Environ. Sci. Technol.* **1996,** *30* (6), 1805-1813; DOI 10.1021/es950012y.

63. Hummel, W.; Berner, U.; Curti, E.; Pearson, F. J.; Thoenen, T. *Nagra/PSI Chemical Thermodynamic Data Base 01/01*; NTB 02-06; NAGRA: Parkland, FL, USA, 2002.

64. Plancque, G.; Maurice, Y.; Moulin, V.; Toulhoat, P.; Moulin, C. On the use of spectroscopic techniques for interaction studies, Part I: complexation between europium and small organic ligands. *Appl. Spectrosc.* **2005,** *59* (4), 432-441.

65. Barkleit, A.; Kretzschmar, J.; Tsushima, S.; Acker, M. Americium(III) and europium(III) complex formation with lactate at elevated temperatures studied by spectroscopy and quantum chemical calculations. *Dalton Trans.* **2014,** *43* (29), 11221-11232; DOI 10.1039/C4DT00440J.

66. Moreau, P.; Colette-Maatouk, S.; Vitorge, P.; Gareil, P.; Reiller, P. E. Complexation of europium(III) by hydroxybenzoic acids: a time-resolved luminescence spectroscopy study. *Inorg. Chim. Acta* **2015,** *432*, 81-88; DOI 10.1016/j.ica.2015.03.036.

67. Marmodée, B.; de Klerk, J. S.; Ariese, F.; Gooijer, C.; Kumke, M. U. High-resolution steady-state and time-resolved luminescence studies on the complexes of Eu(III) with aromatic or aliphatic carboxylic acids. *Anal. Chim. Acta* **2009,** *652* (1-2), 285-294; DOI 10.1016/j.aca.2009.06.006.

68. Kuke, S.; Marmodée, B.; Eidner, S.; Schilde, U.; Kumke, M. U. Intramolecular deactivation processes in complexes of salicylic acid or glycolic acid with Eu(III). *Spectrochim. Acta, Part. A* **2010,** *75* (4), 1333-1340; DOI 10.1016/j.saa.2009.12.080.

69. Szabó, G.; Guczi, J.; Reiller, P. E.; Miyajima, T.; Bulman, R. Effect of ionic strength on complexation of Pu (IV) with humic acid. *Radiochim. Acta* **2010,** *98* (1), 13-18; DOI 10.1524/ract.2010.1683.

70. Hummel, W.; Glaus, M.; van Loon, L. Trace metal-humate interactions. II. The "conservative roof" model and its application. *Appl. Geochem.* **2000,** *15* (7), 975-1001; DOI 10.1016/S0883-2927(99)00100-6.

71. Kinniburgh, D. G.; Milne, C. J.; Benedetti, M. F.; Pinheiro, J. P.; Filius, J.; Koopal, L. K.; van Riemsdijk, W. H. Metal ion binding by humic acid: application of the NICA-Donnan model. *Environ. Sci. Technol.* **1996,** *30* (5), 1687-1698; DOI 10.1021/es950695h.

72. Caceci, M. S. The interaction of humic acid with europium (III). Complexation strength as a function of load and pH. *Radiochim. Acta* **1985,** *39* (1), 51-56; DOI 10.1524/ract.1985.39.1.51.

73. Bertha, E. L.; Choppin, G. R. Interaction of humic and fulvic acids with Eu(III) and Am(III). *J. Inorg. Chem.* **1978,** *40* (4), 655-658; DOI 10.1016/0022-1902(78)80382-0.

74. Torres, R. A.; Choppin, G. R. Europium(III) and americium(III) stability constants with humic acid. *Radiochim. Acta* **1984,** *35* (3), 143-148; DOI 10.1524/ract.1984.35.3.143.

75. Lyklema, J., *Fundamentals of Colloid and Interface Science, Volume I: Fundamentals*. Academic Press Ltd: London, UK, 1995; Vol. I.

76. Domingos, R. F.; Tufenkji, N.; Wilkinson, K. J. Aggregation of titanium dioxide nanoparticles: role of a fulvic acid. *Environ. Sci. Technol.* **2009,** *43* (5), 1282-1286; DOI 10.1021/es8023594.

77. d'Orlyé, F.; Reiller, P. E. Contribution of capillary electrophoresis to an integrated vision of humic substances size and charge characterizations. *J. Colloid Interface Sci.* **2012,** *368* (1), 231-240; DOI 10.1016/j.jcis.2011.11.046.

78. Blaakmeer, J.; Böhmer, M. R.; Cohen Stuart, M. A.; Fleer, G. J. Adsorption of weak polyelectrolytes on highly charged surfaces: poly(acrylic acid) on polystyrene latex with strong cationic groups. *Macromolecules* **1990,** *23* (8), 2301-2309; DOI 10.1021/ma00210a028.

79. Böhmer, M. R.; Evers, O. A.; Scheutjens, J. M. H. M. Weak polyelectrolytes between 2 surfaces: adsorption and stabilization. *Macromolecules* **1990,** *23* (8), 2288-2301; DOI 10.1021/ma00210a027.

80. Weng, L. P.; van Riemsdijk, W. H.; Hiemstra, T. Adsorption of humic acids onto goethite: effects of molar mass, pH and ionic strength. *J. Colloid Interface Sci.* **2007,** *314* (1), 107-118; DOI 10.1016/j.jcis.2007.05.039.

81. Weng, L. P.; van Riemsdijk, W. H.; Hiemstra, T. Adsorption free energy of variable-charge nanoparticles to a charged surface in relation to the change of the average chemical state of the particles. *Langmuir* **2006,** *22* (1), 389-397; DOI 10.1021/la051730t.

82. Saito, T.; Nagasaki, S.; Tanaka, S.; Koopal, L. K. Electrostatic interaction models for ion binding to humic substances. *Colloids Surf. A* **2005,** *265* (1-3), 104-113; DOI 10.1016/j.colsurfa.2004.10.139.

83. Saito, T.; Koopal, L. K.; Nagasaki, S.; Tanaka, S. Electrostatic potentials of humic acid: fluorescence quenching measurements and comparison with model calculations. *Colloids Surf. A* **2009,** *347* (1-3), 27-32; DOI 10.1016/j.colsurfa.2008.10.038.

7. Supporting information

The supporting information contains four Figures and one Table. One Figure shows Eu(III)-SRFA normalized luminescence spectra to the $^5D_0 \rightarrow {}^7F_1$ transition at 0.1 M $NaClO_4$ and $[Eu]_{tot}$ = 1 µM at pH 4, 6 and 7. One Figure shows luminescence decay times of Eu(III) at pH 4, 6 and 7 depending on fulvic concentration for Eu(III) concentrations of 1 µM and 10 µM. One Figure shows the simulation of Eu bound to SRFA and NICA-Donnan parameters using generic parameters. One Figure shows the transformation of asymmetry ration in proportion of Eu(III) bound to the fulvic acid. One Table is showing the NICA-Donnan generic parameters for simulation, and the NICA-Donnan parameters obtained from modeling.

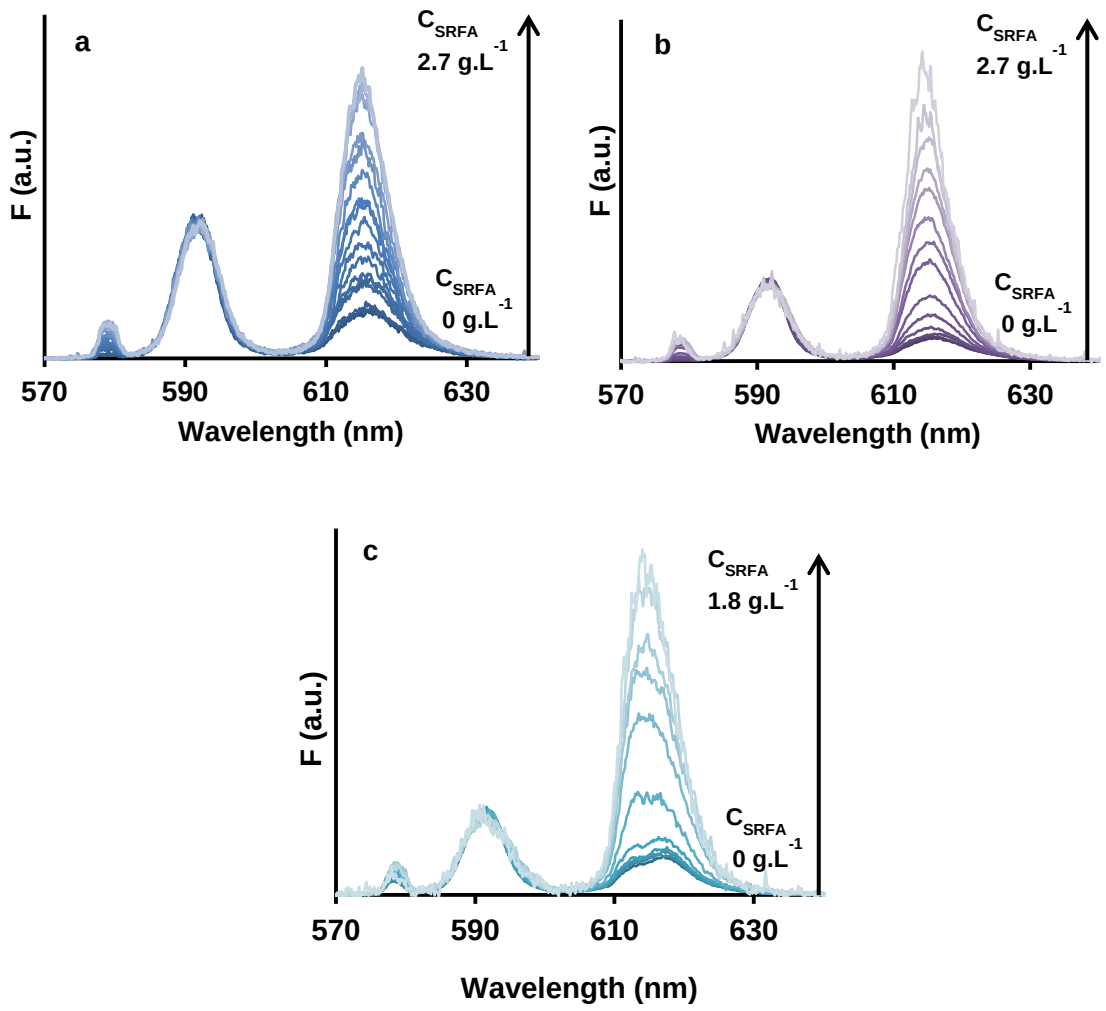

Figure S1. Eu(III)-SRFA normalized luminescence spectra to the $^5D_0 \rightarrow {}^7F_1$ transition at 0.1 M $NaClO_4$ and $C_{Eu(III)}$ = 1 µM, λ_{exc} = 393.7 nm, D = 10 µs, W = 300 µs, 600 lines.mm^{-1} grating, pH 4 (a), pH 6 (b), pH 7 (c).

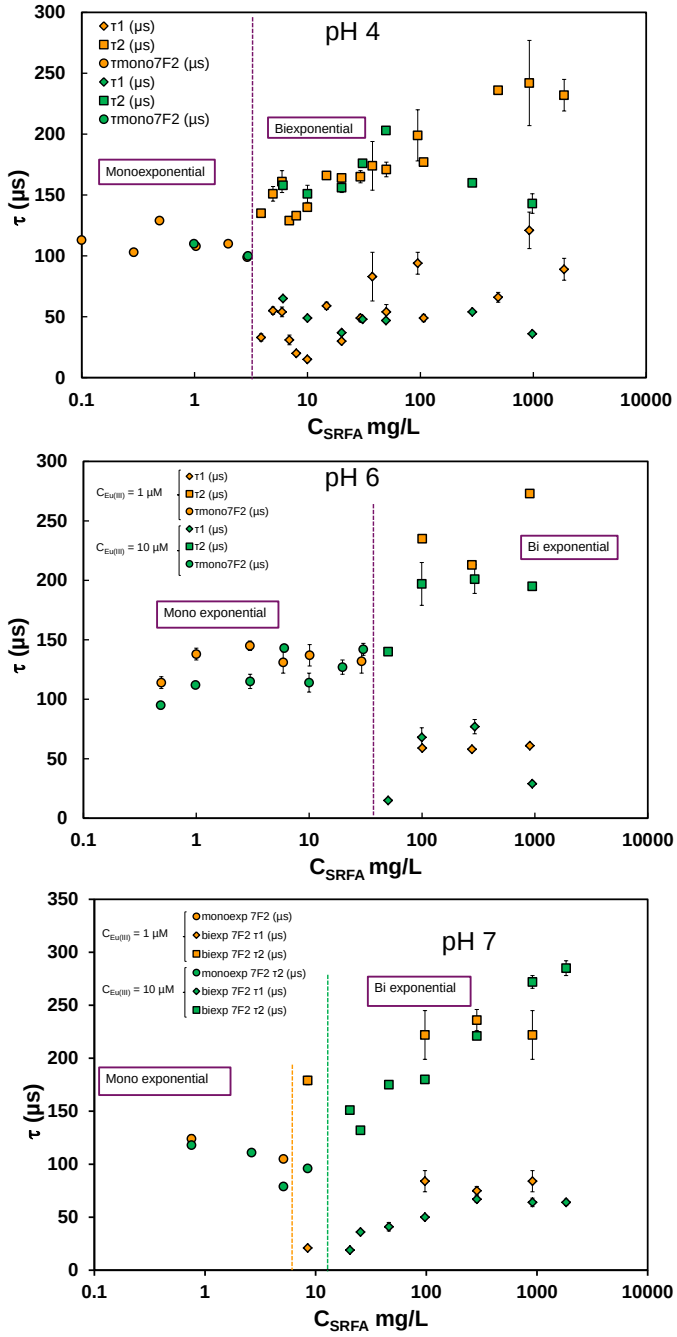

Figure S2. Luminescence decay times of Eu(III) at pH 4 (a), 6 (b) and 7 (c) depending on C_{SRFA} concentration for $C_{Eu(III)}$ of 1 µM (orange symbols), and 10 µM (green symbols) and I = 0.1 M $NaClO_4$. Circles symbols correspond to mono exponential decay times, diamonds and squares correspond to bi-exponential decay times. Dashed lines correspond to the transition between mono and bi exponential decay times (in purple when the transition is the same for the two $C_{Eu(III)}$, in orange for the transition of $C_{Eu(III)}$ of 1 µM, and in green for the transition of $C_{Eu(III)}$ of 10 µM.

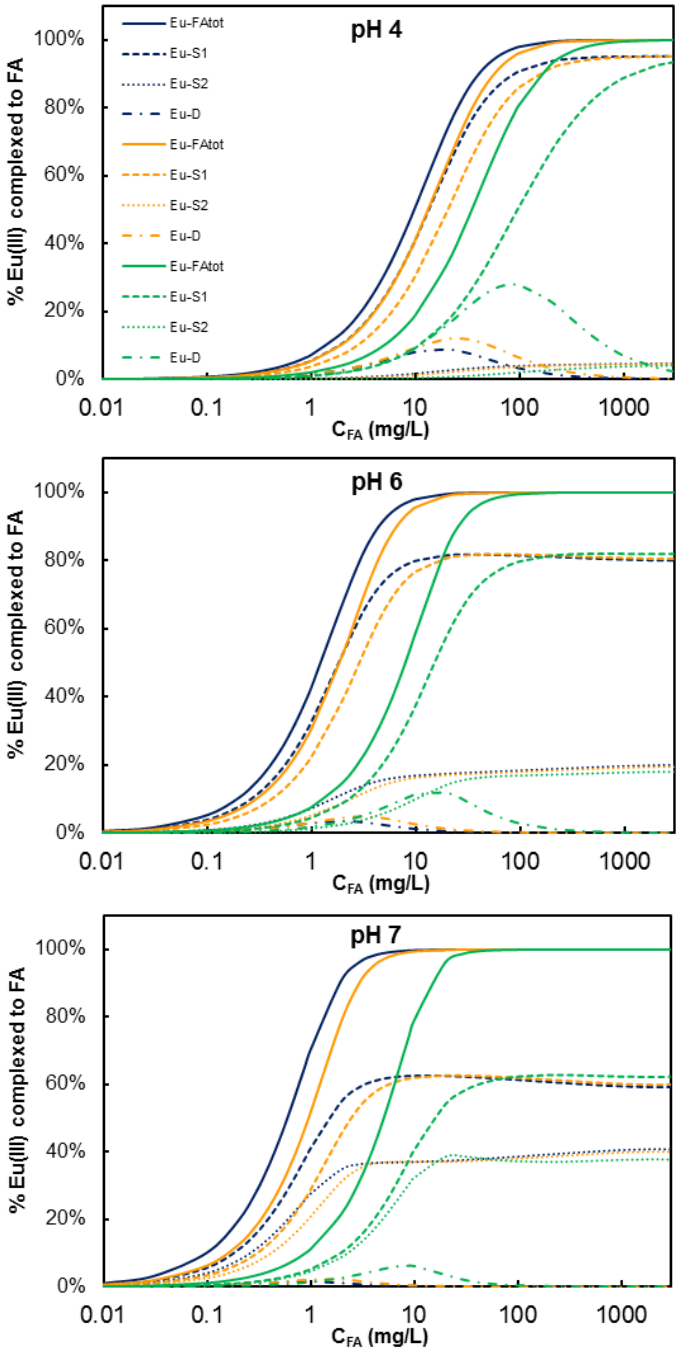

Figure S3. Simulation of the proportion of Eu(III) bound to a generic fulvic acid for $C_{Eu(III)}$ of 0.5 µM (blue lines), 1 µM (orange lines) and 10 µM (green lines) at pH 4 (a), 6 (b), and 7 (c). Simulation of Eu(III) distribution on S_1 sites (dashed lines) and S_2 sites (dotted lines) of SRFA. Solid lines are the sum of S_1 and S_2 sites. Generic NICA-Donnan parameters are given in Table S1.

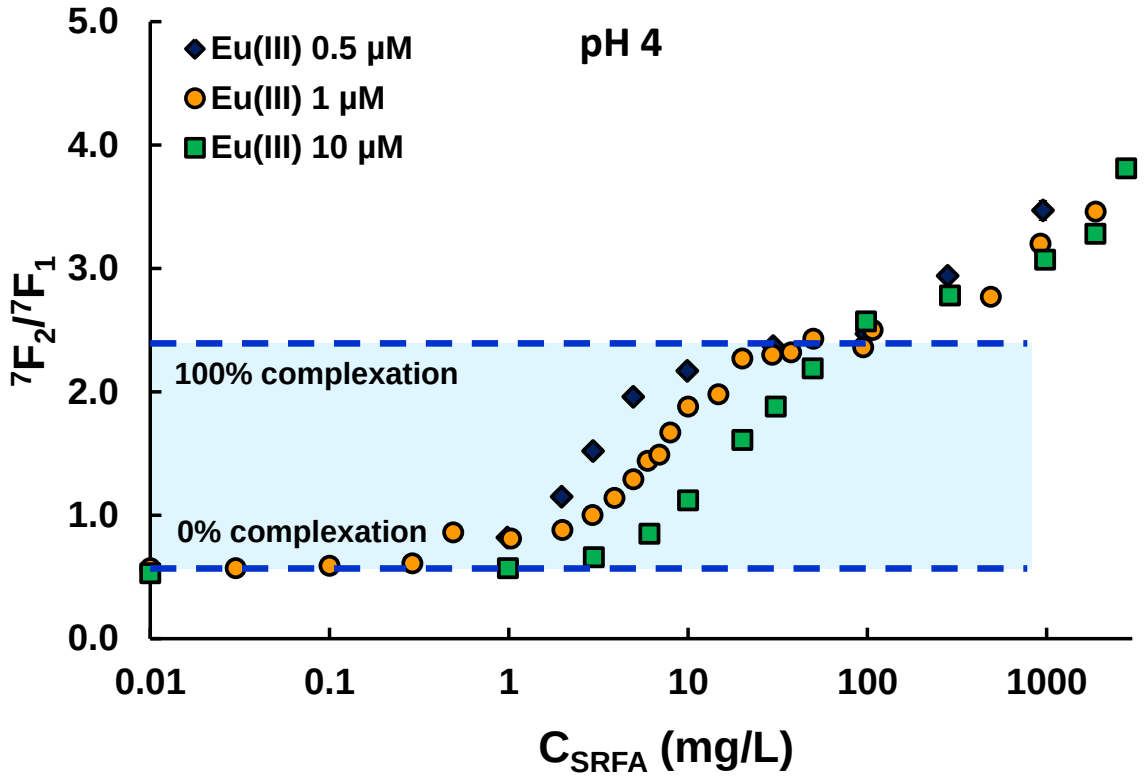

Figure S4. Evolution of asymmetry ratio of Eu(III)-SRFA spectra at pH 4 depending on C_{SRFA} for $C_{Eu(III)}$ of 0.5 (blue diamonds), 1 (orange circles), and 10 µM (green squares) and *I* = 0.1 M $NaClO_4$.

Table S1. NICA-Donnan parameters for proton and Eu(III) binding to a fulvic acid.

	$Q_{max,1}$ (mol.kg$_{FA}^{-1}$)	$n_{M,1}$	$\log_{10}\tilde{K}_{M,1}$	$n_1 \times \log_{10}\tilde{K}_{M,1}$	p_1	$Q_{max,2}$ (mol.kg$_{FA}^{-1}$)	$n_{M,2}$	$\log_{10}\tilde{K}_{M,2}$	$n_{M,2} \times \log_{10}\tilde{K}_{M,2}$	p_2	b	Ref.
H$^+$	5.88	0.66	2.34		0.59	1.86	0.76	8.60		0.70	0.57	*(1)*
Eu^{3+}		0.47	-1.92	-0.90			0.45	5.87	2.64			*(1)*
Eu^{3+}		0.53	-1.11	-0.83			0.40	6.92	2.77			This work

REFERENCES

(1) Milne, C. J.; Kinniburgh, D. G.; Van Riemsdijk, W. H.; Tipping, E. Generic NICA-Donnan model parameters for metal-ion binding by humic substances. *Environ. Sci. Technol.* **2003**, *37*, 958-971.